Carbohydrate Research, 207 (1990) 185–210
Elsevier Science Publishers B.V., Amsterdam

^{13}C-Substituted pentos-2-uloses: synthesis and analysis by ^{1}H- and ^{13}C-n.m.r. spectroscopy

Tapani Vuorinen
Laboratory of Wood Chemistry, Helsinki University of Technology, SF-02150 Espoo (Finland)

and Anthony S. Serianni*
Department of Chemistry and Biochemistry, University of Notre Dame, Notre Dame, Indiana 46556 (U.S.A.)

(Received December 22nd, 1989; accepted for publication March 12th, 1990)

ABSTRACT

D-*erythro*-Pentos-2-ulose and D-*threo*-pentos-2-ulose and their 1-^{13}C- and 2-^{13}C-substituted derivatives have been prepared by oxidizing the corresponding natural and ^{13}C-substituted D-aldopentoses (D-arabinose, D-xylose) with cupric acetate, and purifying the products by chromatography on a cation-exchange resin in the calcium or barium form. The equilibrium compositions of the pentos-2-uloses in $^{2}H_2O$ were determined by ^{13}C-n.m.r. spectroscopy (75 MHz) at 25° and 80°. Among the eighteen possible monomeric acyclic, cyclic, and bicyclic forms, the anomeric pairs of the unhydrated aldopyranoses, aldopyranose endocyclic hydrates, aldofuranose endocyclic hydrates, and ketofuranose exocyclic hydrates were identified on the basis of ^{13}C chemical shifts and ^{13}C–^{1}H and ^{13}C–^{13}C spin-coupling constants. ^{1}H-N.m.r. (300, 500, and 620 MHz) and ^{13}C-n.m.r. (75 MHz) spectroscopic data in one and two dimensions (DQF-COSY, homonuclear 2D-*J*) were used to evaluate the conformational properties of the cyclic structures. The unhydrated pyranoses are highly conformationally homogeneous; the *erythro* and *threo* isomers prefer $^{1}C_4$ and $^{4}C_1$ conformations, respectively. D-*threo*-Pentos-2-ulopyranose hydrate prefers the $^{4}C_1$ conformation whereas the *erythro* isomer exists in both the $^{4}C_1$ and $^{1}C_4$ conformations. The furanoid forms favor structures having quasi-axial anomeric hydroxyl groups and quasi-equatorial exocyclic hydroxymethyl or dihydroxymethyl groups.

INTRODUCTION

Aldos-2-uloses and their deoxy derivatives are important intermediates in oxidation[1] and elimination[2–4] reactions of free aldoses and ketoses. These reactions have important industrial applications, especially in kraft pulping of wood and oxygen bleaching of wood pulp[5a]. Aldos-2-uloses are also useful intermediates in the synthesis of ascorbic acids, particularly analogs of L-ascorbic acid[5b].

The probable structures of the aldos-2-uloses in solution have been discussed in several reviews[2,6–8]. Most of the proposed structures have been inferred from the chemical reactivity of the compounds, although some structural characterization has been based on u.v.-spectroscopic and chromatographic data, rotational behavior, and elemental analysis. G.l.c.–m.s. studies[9,10] of per-*O*-trimethylsilylated aldos-2-uloses have indicated the presence of several isomeric forms[11]. However, these data are not

* Author for correspondence.

0008-6215/90/$ 03.50

unequivocal, as mutarotation can occur during sample derivatization[12]. Free sugars are also known to enolize during per-*O*-trimethylsilylation[13].

At present the preferred method for assessing the solution composition of reducing sugars is high-resolution n.m.r. spectroscopy[12]. ^{13}C-N.m.r. of ^{13}C-substituted compounds has proven very useful for detecting and quantifying minor forms such as acyclic aldehydes and their hydrates[14–21]. Encouraged by the merits of this technique, we conducted a high-resolution n.m.r. study of D-(1-^{13}C)- and D-(2-^{13}C)-*erythro*-pentos-2-ulose (**1**) and -D-*threo*-pentos-2-ulose (**2**). These dicarbonyl sugars may adopt four acyclic, twelve monocyclic, and two bicyclic monomeric structures in aqueous solution (Chart 1). For example, the four acyclic forms of **1** include two monohydrates (**1b**, **1c**), one dicarbonyl form (**1a**), and a dihydrate (**1d**). The twelve monocyclic forms of **1** include two unhydrated ketofuranoses (**1e**, **1f**), two hydrated ketofuranoses ("exocyclic hydrates") (**1g**, **1h**), two unhydrated aldofuranoses (**1i**, **1j**), two hydrated aldofuranoses ("endocyclic hydrates") (**1k**, **1l**), two unhydrated pyranoses (**1m**, **1n**) and two pyranose hydrates (**1o**, **1p**). Dimeric structures are also possible. ^{13}C-Substitution was employed to simplify the assignment of signals to the various forms, and provide additional n.m.r. parameters (^{13}C–^{1}H and ^{13}C–^{13}C spin couplings) for assessing molecular conformation.

Pentos-2-uloses are usually prepared chemically either *via* their phenylosazones or by the direct oxidation of pentoses with cupric acetate[7,8]. We have used the latter method because of its simplicity and relative high yields[22–26], which are desirable in the synthesis of compounds substituted with stable isotopes. Alternatively, biological processes may be used to prepare aldos-2-uloses. Microbial[27] or enzymic[28] oxidation of D-glucose has been used to prepare D-*arabino*-hexos-2-ulose in high yield. Microbial oxidation of D-xylose gives D-*threo*-pentos-2-ulose, but D-arabinose, L-arabinose, D-lyxose, and D-ribose are not oxidized by this method.

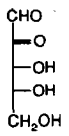

1

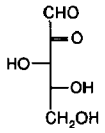

2

EXPERIMENTAL

Materials. — 1-^{13}C- And 2-^{13}C-substituted D-arabinose and D-xylose were obtained from Omicron Biochemicals, Inc. D-Arabinose, D-ribose, and hydroxylamine hydrochloride were purchased from the Sigma Chemical Company. D-Lyxose was obtained from the Aldrich Chemical Company, and D-xylose from the Nutritional Biochemicals Corporation. Cupric acetate, 3% hydrogen peroxide, magnesium chloride, sodium hydroxide, sulfuric acid, potassium iodide, and 0.1N standard iodine solution were from the Fisher Scientific Company. Ammonium molybdate was from the J. T. Baker Chemical Company, and *N,O*-bis(trimethylsilyl)trifluoroacetamide (BSTFA) containing 1% chlorotrimethylsilane was from the Pierce Chemical Compa-

ny. Deuterium oxide (^2H_2O, 99.9 atom-% ^2H) was purchased from Cambridge Isotope Laboratories.

Instrumentation. — High-resolution FT ^{1}H-n.m.r. spectra at 620 MHz were obtained at the NMR Facility for Biomedical Studies, Department of Chemistry, Carnegie–Mellon University, Pittsburgh, PA.

High-resolution ^{1}H-n.m.r. spectroscopy at 300 MHz and ^{13}C-n.m.r. spectroscopy at 75 MHz were performed on a General Electric GN-300 FT-n.m.r. spectrometer in the Department of Chemistry and Biochemistry, University of Notre Dame. Quantitative ^{1}H-decoupled ^{13}C-n.m.r. spectra were obtained without nuclear Overhauser enhancement (n.O.e.), using a relaxation delay of 20 s between acquisitions. ^{1}H-Coupled

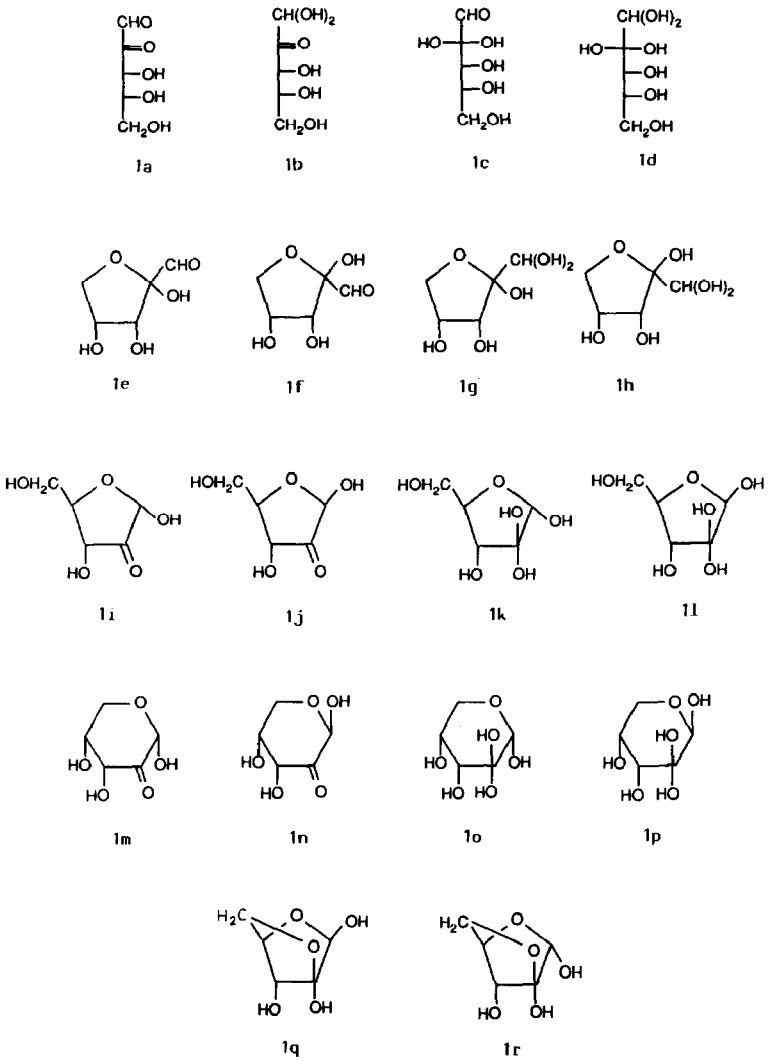

Chart 1. Compounds **2a–r** are the C-3 epimers of **1a–r**.

^{13}C-n.m.r. spectra were obtained with n.O.e. by gating the ^{1}H-decoupler off during data acquisition.

Chemical shifts are referenced to sodium 3-(trimethylsilyl)-propane-1-sulfonate (DSS). Carbon-13 shifts were measured from C-1 of external α-D-(1-^{13}C)mannopyranose at 95.5 p.p.m., and are accurate to ±0.1 p.p.m. Proton shifts were measured from HOD at 4.80 p.p.m., and are accurate to ±0.01 p.p.m. *J*-Values are accurate to ±0.1 Hz.

The resolution of non-quantitative ^{1}H- and ^{13}C-n.m.r. spectra was enhanced by applying a double-exponential apodization function to free-induction decays (FIDs) prior to Fourier transformation. FIDs for quantitative ^{13}C FT-n.m.r. spectra were processed with an exponential multiplication function to increase the number of data points defining the signals.

Homonuclear 2D *J*-spectra and DQF-COSY spectra were obtained on a Varian VXR-500 500 MHz n.m.r. spectrometer using software supplied by Varian Instruments. For *J*-spectra, a 4K × 4K matrix was obtained over a sweepwidth of ~2500 Hz, and sine bell functions were applied to the FIDs in both t_1 and t_2 dimensions; DQF-COSY spectra were obtained with a 2K × 2K matrix, and FIDs were processed similarly.

Gas-liquid chromatography (g.l.c.) was performed on a Varian Model 1400 gas chromatograph equipped with a glass column (6 ft) packed with 3% OV-17 on 100–120 mesh Chromosorb W-HP obtained from Alltech Associates.

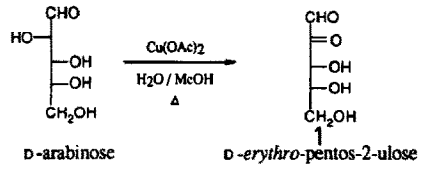

D-arabinose — 1 — D-*erythro*-pentos-2-ulose

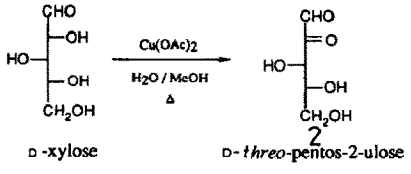

D-xylose — 2 — D-*threo*-pentos-2-ulose

Scheme 1.

Preparation of D-erythro-*pentos-2-ulose* (1). — As shown in Scheme 1, D-arabinose (1.00 g, 6.7 mmol) was dissolved in 96% aqueous methanol (60 mL) and heated under reflux in a two-necked round-bottom flask. Cupric acetate monohydrate (4.60 g, 23.1 mmol) was added and the mixture was heated for an additional 15 min. The reaction mixture was cooled (cold water) and centrifuged, the supernatant was removed, the precipitate was mixed with 96% aqueous methanol (30 mL), and this suspension was centrifuged. The combined supernatants were applied to a column (2.0

× 12 cm) of Dowex HCR-W2 (20–50 mesh) cation exchange resin in the H^+ form, which was washed with 96% aqueous methanol before sample loading. The column was eluted with 96% aqueous methanol (300 mL) until the phenol–sulfuric acid assay[29a] was negative. The combined eluates were concentrated in vacuo at 30°, and the resulting syrup was diluted with water (20 mL) and concentrated two additional times to remove acetic acid. After the last evaporation, the syrup was dissolved in water (20 mL), the solution was boiled for a few minutes to decompose any dimers formed during concentration, and cooled. It was then applied to a column (4.0 × 106 cm) of Dowex 50W-X8 (200–400 mesh) cation-exchange resin in the Ca^{2+} form, and the product (**1**) was eluted with distilled water[29b]. The elution volume of D-*erythro*-pentos-2-ulose (**1**) was 1450 mL, so it was well separated from D-arabinose (elution volume 800 mL) and reaction by-products. The yield of **1** was 29% as determined by the titrimetric method described below.

Preparation of D-threo-*pentos-2-ulose* (**2**). — As shown in Scheme 1, D-xylose (1.00 g, 6.7 mmol) was dissolved in 96% aqueous methanol (60 mL) and heated under reflux in a two-necked round-bottom flask. Cupric acetate monohydrate (4.00 g, 20.1 mmol) was added and the mixture was heated for an additional 10 min. The inorganic precipitate was removed by centrifugation, the supernatant was deionized by passage through the cation-exchange column, and the eluate was made ready for preparative ion-exchange chromatography as described above for **1**. The reaction mixture was applied to a column (3.8 × 104 cm) of Dowex 50W-X8 (200–400 mesh) cation-exchange resin in the Ba^{2+} form, and the product (**2**) was eluted with distilled water[30]. D-*threo*-Pentos-2-ulose (**2**) did not separate completely from D-xylose (the elution volumes were 840 mL and 690 mL, respectively), necessitating rechromatography of the middle fraction. The yield of **2** was 53% as determined by the titrimetric method described below.

Quantification of pentos-2-uloses **1** *and* **2**. — Aqueous solutions of **1** and **2** were analyzed by oxidation with standard hydrogen peroxide, which effects cleavage of the C-1–C-2 bond[31]. To a beaker were added 0.1M sodium hydroxide (10 mL), 0.1M hydrogen peroxide–0.02M magnesium chloride (1 mL) (exact concentration of H_2O_2 determined by titration against standard iodine), and the sample containing 20–30 μmol of the pentos-2-ulose. The solution was stirred for 2 min at ambient temperature after which were added distilled water (40 mL), concentrated sulfuric acid (2 mL), potassium iodide (0.2 g), 3 drops of 3% (w/v) aqueous ammonium molybdate, and several drops of starch solution. The solution was titrated with 0.025M sodium thiosulfate (exact concentration determined by titration with standard iodine solution) until the color of the starch–iodine complex disappeared[32]. The amount of pentos-2-ulose was calculated from the volume of hydrogen peroxide consumed during the oxidation.

*Gas–liquid chromatography (g.l.c.) of per-*O*-trimethylsilylated oximes of pentoses and pentos-2-uloses.* — An aqueous sample containing 1–2 mg of compound was evaporated to a syrup and 0.5 mL of anhydrous pyridine containing 5 mg of hydroxylamine hydrochloride was added. The solution was incubated at ambient temperature for 2 h, or at 100° for 5–10 min, after which 0.25 mL of BSTFA containing 1% Me_3SiCl

was added. This solution was incubated at ambient temperature for ~20 min before analysis by g.l.c.[33,34].

The per-*O*-trimethylsilylated compounds were separated on a packed glass column containing 3% OV-17 on Chromosorb W-HP. Temperature was programmed at 10°.min^{-1} from 100° to 200°, followed by 5 min at 200°. Retention times (in min) were as follows: D-arabinose, 8.05; D-ribose, 8.35; D-*erythro*-pentos-2-ulose, 8.5 and 8.95; D-lyxose, 7.7 and 8.1; D-xylose, 8.2; and D-*threo*-pentos-2-ulose, 8.75 and 9.05.

RESULTS AND DISCUSSION

Synthesis of pentos-2-uloses **1** *and* **2**. — D-Pentoses consume two molar equivalents of cupric ions when converted into D-pentos-2-uloses. Cuprous ions partly precipitate as the oxide[22-26] and the solution becomes acidic due to the formation of acetic acid. Acetic acid catalyzes the oxidation; the reaction rate was retarded when neutralizing agents (*e.g.* sodium bicarbonate) were added to the reaction mixture.

The oxidation rates of pentoses increased in the order D-ribose < D-arabinose < D-xylose < D-lyxose. The pyranoid forms appear most easily oxidized, but the present experiments were not sufficient to determine which pentopyranose configurations and conformations are most amenable to oxidation. When D-ribose was mixed with cupric acetate a viscous solution or gel resulted, suggesting that D-ribose forms a stable complex with cupric ions. The slow oxidation rate of D-ribose may be partly due to this complex formation.

At least two molar equivalents of cupric acetate are needed to obtain a good yield of pentos-2-uloses because cupric ions are consumed in side reactions (*e.g.* oxidation of pentos-2-uloses) or form unreactive complexes with pentoses, especially D-ribose. In the present experiments the optimum charge of cupric acetate was 2.5–3.0 molar equivalents for D-xylose and D-lyxose, 3.0–3.5 for D-arabinose, and 4 for D-ribose. Other workers have used 3.2–4.2 molar equivalents of cupric acetate to oxidize D-xylose[22-26].

Aldos-2-uloses are difficult to purify when prepared by the cupric acetate method[8], hence the phenylosazone method of preparation is often applied when purity is essential[7]. In this work, the pentos-2-uloses were purified by ion-exchange chromatography. D-*erythro*-Pentos-2-ulose (**1**) was isolated in high purity by chromatography on Dowex 50-X8 (200–400 mesh) cation exchange resin in the calcium form. In contrast, D-*threo* -pentos-2-ulose (**2**) could not be separated from D-xylose on this calcium resin, but separation was possible on the same resin in the barium form. The retention volume of **2** was, however, relatively small and therefore it still contained minor impurities.

Several alternative ion-exchange resins were tested but did not yield **2** in greater purity. Cation and anion exchange resins were tested with aqueous ethanol as the eluent[35] but the pentos-2-ulose eluted as a very broad peak, which prevented purification. Pentos-2-uloses were separated on Dowex 1-X8 (200–400 mesh) anion exchange resin in the carbonate/hydrogencarbonate form (aldos-2-uloses are much more acidic than aldoses)[4], but it was necessary to elute the compounds very rapidly at a low temperature in order to minimize degradation. The separation of pentos-2-uloses on

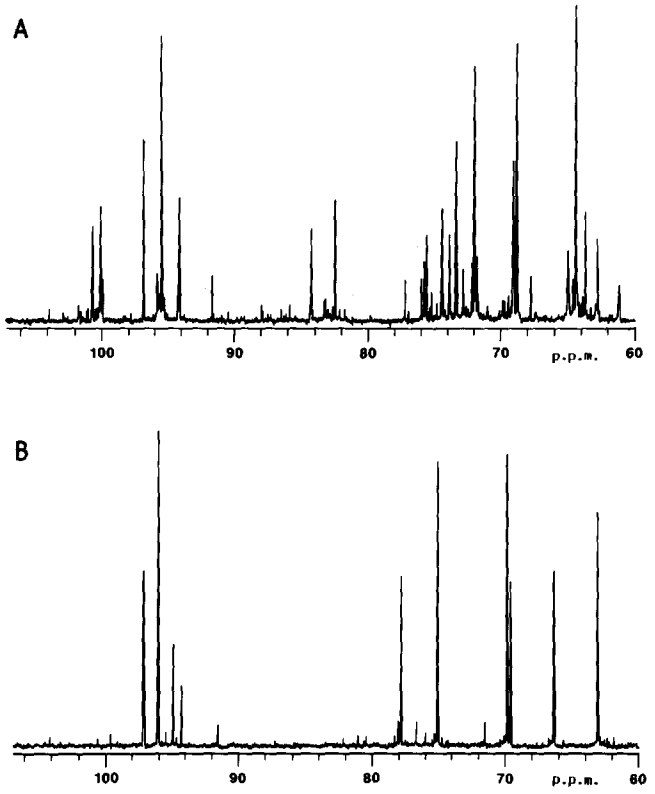

Fig. 1. ^{1}H-Decoupled ^{13}C-n.m.r. spectra (75 MHz) at ambient temperature. A, D-*erythro*-pentos-2-ulose (1); B, D-*threo*-pentos-2-ulose (2).

Dowex 1-X8 (200–400 mesh) resin in the hydrogensulfite form was not practical because of the large retention volumes of the compounds (the complexes formed between pentos-2-uloses and hydrogensulfite are very stable)[36].

^{13}C-N.m.r. spectra of pentos-2-uloses. — The ^{13}C-n.m.r. spectrum of D-*threo*-pentos-2-ulose in $^{2}H_2O$ contains two dominant sets of five signals and some minor signals (Fig. 1B). In contrast, the spectrum of D-*erythro*-pentos-2-ulose (Fig. 1A) is more complicated, indicating the presence of several major forms. The spectra of the 1-^{13}C- and 2-^{13}C-substituted compounds revealed the presence of additional minor forms which were not detected in spectra of the natural-abundance samples (Figs. 2 and 3).

Preparations of D-*erythro*-pentos-2-ulose were highly pure, and no signals attributable to impurities were detected in spectra of the ^{13}C-substituted compounds. However, some signal intensities depended on sample concentration, suggesting the presence of dimeric or oligomeric forms. At a concentration of 1M these forms accounted for $\leqslant 10\%$ of the total mixture.

^{13}C-N.m.r. spectra of ^{13}C-substituted D-*threo*-pentos-2-uloses contained signals for impurities at 160–170 p.p.m. (1-^{13}C) and at 100–115 and 170–180 p.p.m. (2-^{13}C).

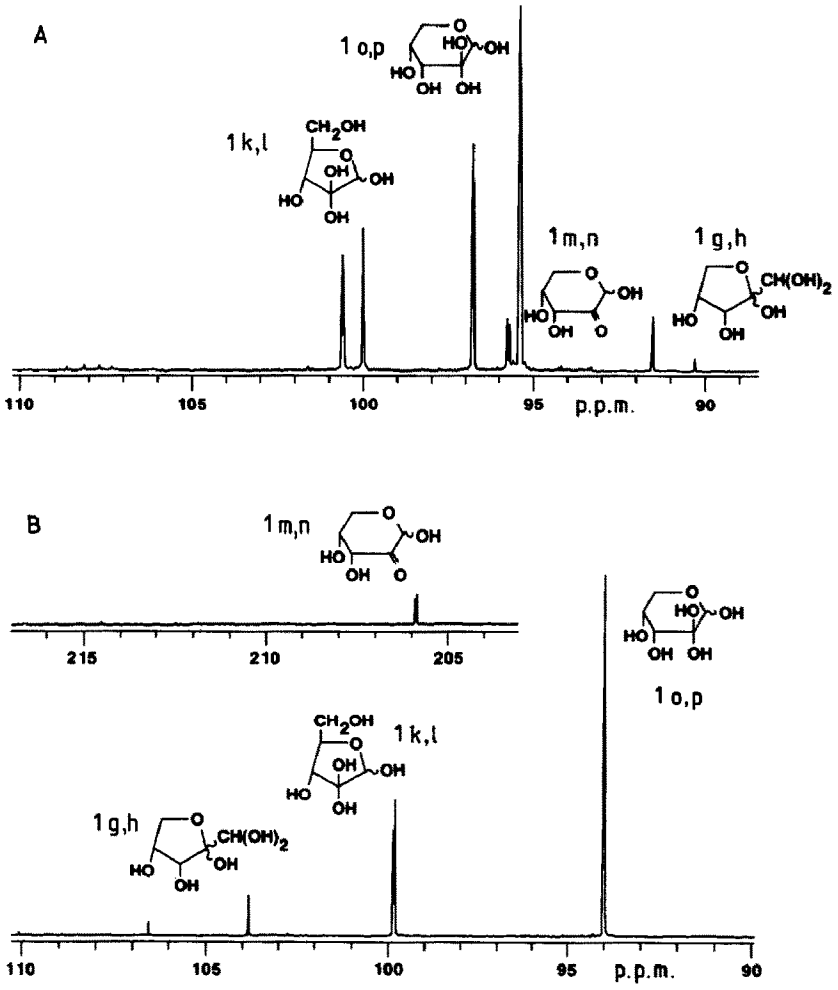

Fig. 2. ^{1}H-Decoupled ^{13}C-n.m.r. spectra (75 MHz) at ambient temperature. A, D-(1-^{13}C)*erythro*-pentos-2-ulose; B, D-(2-^{13}C)*erythro*-pentos-2-ulose.

These impurities were degradation products, since they increased in abundance with time at elevated temperatures. Spectra of ^{13}C-substituted D-*threo*-pentos-2-uloses also revealed the presence of dimeric forms (< 10% at 1M concentration).

a) Anomeric carbons (C-1 and C-2). The possible monomeric structures of D-*erythro*-pentos-2-ulose (**1**) and, by extension, D-*threo*-pentos-2-ulose (**2**) are depicted in Chart 1. The chemical shifts of the anomeric C-1 and C-2 carbons, in combination with $J_{C\text{-}1,H}$ and $J_{C\text{-}2,H}$ values, are key parameters in making structural assignments.

C-1 and C-2 of the two major forms of **1** and **2** resonate at 94–97 p.p.m., indicating that the structures containing these carbons are cyclic hydrates (Table I). On the basis of $^{1}J_{C\text{-}1,H\text{-}1} \sim 165.4 \pm 2.6$ Hz (Table II)[37–39], these structures were identified as the pyranose hydrates **1o**, **1p**, **2o**, and **2p**; aldofuranose endocyclic hydrates (**1k**, **1l**, **2k**, **2l**) have larger $^{1}J_{C\text{-}1,H\text{-}1}$ values ($\sim$172 Hz)[19,20,40,41], and the C-1 carbons of ketofuranose exocyclic hydrates (**1g**, **1h**, **2g**, **2h**) typically resonate at 90–92 p.p.m.[42–45].

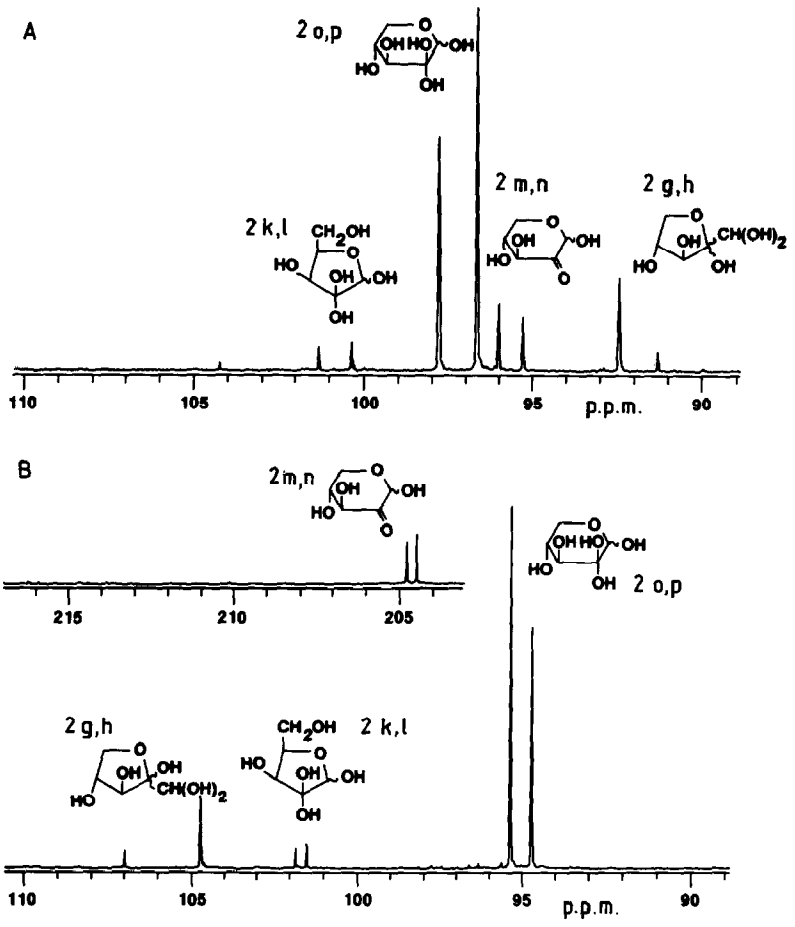

Fig. 3. ^{1}H-Decoupled ^{13}C-n.m.r. spectra (75 MHz) at 80°. A, D-(1-^{13}C)*threo*-pentos-2-ulose; B, D-(2-^{13}C)-*threo*-pentos-2-ulose.

TABLE I

Carbon-13 and proton chemical shifts of D-pentos-2-ulopyranose endocyclic hydrates

Nucleus	α-erythro **1o**	β-erythro **1p**	α-threo **2o**	β-threo **2p**
C-1	96.8	95.4	96.0	97.1
C-2	94.0	94.0	94.9	94.2
C-3	73.3	71.8	75.0	77.8
C-4	68.9	68.6	69.8	69.6
C-5	64.9	64.3	63.1	66.3
H-1	4.66	4.89	4.93	4.65
H-3	3.78	3.89	~3.77	3.51
H-4	3.97	4.02	~3.77	~3.75
H-5*R*	3.67	3.93	~3.77	3.98
H-5*S*	3.91	3.68	~3.77	3.36

The configurations at C-1 of **2o** and **2p** were assigned from the magnitudes of $^1J_{C\text{-}1,H\text{-}1}$, using correlations derived previously for the structurally related aldohexopyranoses[37–39]. The values of $^1J_{C\text{-}1,H\text{-}1}$ for **1o** and **1p** were similar, and their assignments were substantiated by calculation of the conformational free energies (the β anomer is more stable)[46].

^{13}C-N.m.r. spectra of **1** and **2** enriched with ^{13}C at C-1 contain two prominent signals in the aldehyde hydrate region (90–92 p.p.m.)[14,15,17–21]. On the basis of signal intensities, the corresponding C-2 resonances of the 2-^{13}C-substituted derivatives were located at 104–107 p.p.m. Since 2-ketofuranose anomeric carbons typically resonate in this latter region[42–45], these signals were assigned to the ketofuranose exocyclic hydrates **1g**, **1h**, **2g**, and **2h** (Table III). The C-2 signal intensities of the ketofuranose exocyclic hydrates were different, and on the basis of their larger $^3J_{C\text{-}1,H\text{-}3}$ values (Table IV)[45,47,48] the major anomers were assigned configurations **1g** and **2h**, which have C-1 and H-3 *cis*. The same assignment was made on the basis of anomeric-carbon chemical shifts. In the structurally related 2-pentulofuranoses, C-2 of anomers having O-2,O-3 *cis* is more shielded than C-2 of anomers having O-2,O-3 *trans*. By analogy, C-2 of **1g** and **2h** are expected to be more shielded than C-2 of **1h** and **2g**. Thus, anomers of ketofuranose exocyclic hydrates having C-1 and O-3 *trans* are more stable than those anomers having these substituents *cis*[12,50], which is consistent with the anomeric distribution observed in 2-pentulofuranoses.

^{13}C-N.m.r. spectra of **1** and **2** contain a third pair of C-2 signals in the anomeric region. In aqueous solutions of **1** these signals were the second most intense signals. Because the corresponding C-1 signals are also found in the anomeric region (Table V), two types of structures were possible, namely the aldofuranose endocyclic hydrates **1k**, **1l**, **2k**, and **2l**, and the bicyclic difuranoses **1q**, **1r**, **2q**, and **2r**. It is likely that C-1 in the bicyclic structures would be coupled strongly to H-3 and/or H-4[47,48]. Since strong couplings were not observed in the ^{1}H-coupled ^{13}C-spectrum (Table VI), the observed anomeric signals were assigned to the aldofuranose endocyclic hydrates. The *threo* isomers **2k** and **2l** were not as abundant as **1k** and **1l** because of the unfavorable *cis* interaction between O-3 and C-5 in the former[12,50].

The assignment of the anomeric carbon signals of the aldofuranose endocyclic hydrates to specific anomers was based on coupling constants that are conformation-dependent and is discussed further below. This analysis indicates that **1l** is the more abundant of the aldofuranose endocyclic hydrates having the *erythro* configuration.

The ^{13}C-n.m.r. spectra of 2-^{13}C-substituted **1** and **2** contain two prominent signals in the carbonyl region (Figs 2B and 3B). The corresponding C-1 signals in 1-^{13}C-substituted **1** and **2** are in the anomeric region (Table VII). The $^1J_{C\text{-}1,H\text{-}1}$ values (Table VIII) for the two forms were different, and suggest that these forms are the anomeric unhydrated pyranoses **1m**, **1n**, **2m**, and **2n**.

Several minor carbonyl signals were also detected in the ^{13}C spectra of **1** and **2**; three peaks (0.2–0.3% each) were observed at 210, 213, and 214 p.p.m. in the spectrum of D-(2-^{13}C)*threo*-pentos-2-ulose at 80°. These signals may be due to the unhydrated aldofuranoses **2i** and **2j** and the acyclic hydrate **2b**. In the ^{13}C-n.m.r. spectrum of

TABLE II

Spin–spin coupling constants in D-pentos-2-ulopyranose hydrates

Coupled nuclei	*J (Hz)*			
	α-erythro **1o**	β-erythro **1p**	α-threo **2o**	β-threo **2p**
H-3, H-4	3.4	3.3		9.2
H-4, H-5*R*	2.7	3.6		5.4
H-4, H-5*S*	5.1	6.8		10.4
H-5*R*, H-5*S*	−12.4	−11.9		−11.6
C-1, H-1	164.3	166.3	168.6	162.5
C-1, H-3	1.7	1.9		0
C-1, H-5*R*	4.2	6.1		10.1
C-1, H-5*S*	7.3	4.7		2.9
C-2, H-1	1.8	0	2.7	4.2
C-2, H-3	3.3	3.9	2.0	2.0
C-2, H-4		3.4		0
C-3, H-3	144.5	146.0	144.3	147.1
C-4, H-4	148.0	147.1	148.5	148.3
C-5, H-5	143.2 149.8	146.7	147.1	141.2 150.5
C-1, C-2	52.0	53.4	54.9	51.4
C-1, C-3	4.5	2.0	2.0	6.0
C-1, C-4	0	0	0	0
C-1, C-5	0	0	2.0	0
C-2, C-3	44.1	44.7	43.1	43.8
C-2, C-4	0	0	1.2	1.4
C-2, C-5	0	br[a]	br[a]	0

[a] Denotes broadened signal.

D-(2-^{13}C)*erythro*-pentos-2-ulose, two peaks (0.7% and 2.0%) were observed at ~215 p.p.m. at 80°. The larger signal was also detected at 25° (0.3%). These signals may originate from the unhydrated aldofuranoses **1i** and **1j** and the acyclic hydrate **1b**. The presence of **1b** is also supported by a prominent peak (~2%) at 94 p.p.m. in the spectrum of D-(2-^{13}C)*erythro*-pentos-2-ulose at 80°.

The carbonyl carbons of cyclopentanones resonate ~10 p.p.m. downfield from the carbonyl carbons of cyclohexanones and acyclic ketones[51]. On the basis of this observation the C-2 carbons of the unhydrated aldofuranoses are expected to resonate at ~215 p.p.m. On the other hand the C-2 chemical shifts of the acyclic hydrates **1b** and **2b** (~215 p.p.m.) should be similar to those of the unhydrated pyranoses (~206 p.p.m.), but they differ.

In the ^{13}C-n.m.r. spectra of D-(1-^{13}C)*erythro*- and D-(1-^{13}C)*threo*-pentose-2-ulose, weak signals (0.1%) were observed at 200 p.p.m. (one peak) and 201–202 p.p.m. (two peaks), respectively. These chemical shifts are typical of free aldehydes[14,15,17–21] and may indicate the presence of the ketofuranoses **1e**, **1f**, and **2f**.

b) Non-anomeric carbons (C-3 to C-5). The non-anomeric carbon signals of **2o** and **2p**, and **1k**, **1l**, **1o**, and **1p** (Tables I and V) were differentiated on the basis of their significantly different signal intensities. The C-3 signals were assigned on the basis of $^{1}J_{C\text{-}2,C\text{-}3}$ values measured on 2-^{13}C-substituted compounds (Tables II and VI). The C-5 signals were at higher fields than the other signals and were triplets in the absence of

TABLE III

Carbon-13 and proton chemical shifts of ketofuranose exocyclic hydrates of pentos-2-uloses

Nucleus	*Chemical shift (p.p.m.)*			
	α-erythro **1g**	β-erythro **1h**	α-threo **2g**	β-threo **2h**
C-1	91.5	90.3	90.2	91.5
C-2	103.8	106.5	106.5	104.0
C-3	72.0			78.0
C-4	71.6			76.6
C-5	72.7			71.5
H-1	4.93	5.11		4.98
H-3	4.20			4.15
H-4	4.33			4.36
H-5*R*	4.00			4.20
H-5*S*	3.91			3.69

TABLE IV

Spin–spin coupling constants of ketofuranose exocyclic hydrates of pentos-2-uloses

Coupled nuclei	J *(Hz)*			
	α-erythro **1g**	β-erythro **1h**	α-threo **2g**	β-threo **2h**
H-3, H-4	5.4			5.1
H-4, H-5*R*	4.9			6.0
H-4, H-5*S*	3.1			~5.0
H-5*R*, H-5*S*	−10.0			−9.6
C-1, H-1	163.4	166.6	166.3	163.5
C-1, H-3	2.4	0	0	2.4
C-2, H-1	0	1.2		0
C-2, H-3	0			0
C-2, H-5*S*				4.5
C-1, C-3	3.6			3.9
C-1, C-4	0			1.9
C-1, C-5	br[a]			~1
C-2, C-3	44.0			~44
C-2, C-4	1.4			~3
C-2, C-5	0			0

[a] Denotes broadened signal.

TABLE V

Carbon-13 and proton chemical shifts of aldofuranose endocyclic hydrates of pentos-2-uloses

Nucleus	*Chemical shift (p.p.m.)*			
	α-erythro **1k**	β-erythro **1l**	α-threo **2k**	β-threo **2l**
C-1	100.6	100.0	99.6	100.5
C-2	99.85	99.81	100.9	101.4
C-3	75.5	74.3		
C-4	84.2	82.4		
C-5	62.7	63.6		
H-1	5.14	5.01		
H-3	3.84	3.95		
H-4	4.05	3.82		
H-5*R*	3.69	3.68		
H-5*S*	3.80	3.81		

TABLE VI

Spin–spin coupling constants of aldofuranose endocyclic hydrates of pentos-2-uloses

Coupled nuclei	*J (Hz)*			
	α-erythro **1k**	β-erythro **1l**	α-threo **2k**	β-threo **2l**
H-1, H-3	0.6	0		
H-3, H-4	6.5	7.2		
H-4, H-5*R*	5.6	6.6		
H-4, H-5*S*	3.4	3.2		
H-5*R*, H-5*S*	−12.3	−12.8		
C-1, H-1	172.2	172.7	175.9	172.8
C-1, H-3	1.3	0	1.7	3.2
C-1, H-4	0	0	0	0
C-2, H-1	0	0	0	0
C-2, H-3	3.3	2.3	3.5	4.2
C-2, H-4	0	0	0	0
C-3, H-3	147.9	147.5		
C-4, H-4	148.6	149.6		
C-5, H-5	143.3	143.5		
C-1, C-3	6.7	7.0		
C-1, C-4	0	0		
C-1, C-5	br[a]	0		
C-2, C-3	46.1	45.7		
C-2, C-4	3.5	3.3		
C-2, C-5	2.3	2.5		

[a] Denotes broadened signal.

broadband ^{1}H-decoupling. The C-4 signals were assigned by difference, although these signals have characteristic features that may be used for assignment. The C-4 chemical shift is essentially unaffected by anomeric configuration in pyranose chair conformers; the C-4 carbon shifts of pyranose anomers are very similar if the conformational equilibria for each anomer are similar[51]. In the aldofuranoses **1k** and **1l**, O-4 participates in ring formation, causing a significant downfield shift of the C-4 resonance[17,19,21,49,52].

The chemical shifts of the non-anomeric carbons of **2h** (Table III) are similar to those of *β*-D-*threo*-2-pentulofuranose[45]. The assignment for each carbon was verified by consideration of the $^1J_{C\text{-}2,C\text{-}3}$ value (Table IV), and by the observed signal multiplicity in the ^{1}H-coupled ^{13}C-spectrum. In **2h**, C-5 is more shielded than C-4 (and C-3).

The signal intensities of the non-anomeric carbons of **1g**, **1m**, and **1n** are similar, but their ^{13}C chemical shifts differ enough to enable their assignment (Tables III and VII). The chemical shifts of the non-anomeric carbons of **1g** are similar to those of *α*-D-*erythro*-2-pentulofuranose[45], as expected. The C-3 signals of **1m** and **1n** were assigned on the basis of the $^2J_{C\text{-}1,C\text{-}3}$ (ref. 45) and $^1J_{C\text{-}2,C\text{-}3}$ values (Table VIII). Because **1m** and **1n** exist in the $^1C_4$ conformation, C-3 of the *β* anomer (**1n**) is more shielded than C-3 of the *α* anomer (**1m**) by the anomeric hydroxyl group[52], axial in the former case. The axial anomeric hydroxyl group of **1n** is also responsible for the shielding of C-5 relative to C-5 of **1m**. As expected, the C-4 resonances of **1m** and **1n** are very close, but C-4 of **1m** appears more shielded[52]. C-3 and C-4 of **1m** and **1n** are considerably deshielded (3–6 p.p.m.) relative to C-3 and C-4 of *α*- and *β*-D-arabinopyranose[52], probably because of the presence of the free carbonyl group[51].

One-dimensional ^{1}H-n.m.r. spectra of the pentos-2-uloses. The anomeric-proton signals of the major forms of **1** and **2** were well resolved at 300 MHz, whereas most of the non-anomeric proton signals were resolved at 620 MHz (Fig. 4).

The H-3, H-4, H-5*R*, and H-5*S* protons of **2o** have similar chemical shifts,

TABLE VII

Carbon-13 and proton chemical shifts of D-pentos-2-ulopyranoses

Nucleus	*Chemical shift (p.p.m.)*			
	α-erythro **1m**	*β*-erythro **1n**	*α*-threo **2m**	*β*-threo **2n**
C-1	95.75	95.67	95.4	94.6
C-2	205.88	205.95	203.9	203.5
C-3	77.1	74.3		
C-4	75.6	75.9		
C-5	67.6	64.5		
H-1	5.26	5.19		
H-3	4.73	4.91		
H-4	~4.45	~4.45		
H-5*R*	4.09	4.47		
H-5*S*	4.04	3.85		

TABLE VIII

Spin–spin coupling constants of D-pentos-2-ulopyranoses

Coupled nuclei	J *(Hz)*			
	α-erythro **1m**	β-erythro **1n**	α-threo **2m**	β-threo **2n**
H-1, H-3	1.1	0		
H-3, H-4	4.2	3.9		
H-4, H-5*R*	1.1	~1.2		
H-4, H-5*S*	2.1	2.2		
H-5*R*, H-5*S*	−13.3	−12.9		
C-1, H-1	164.1	174.0	174.8	165.5
C-1, H-3	0	0	0	0
C-1, H-5*R*	4.3	2.2	7.2	10.0
C-1, H-5*S*	9.9	8.1	2.6	4.0
C-2, H-1	3.6	1.8	~1	~3.5
C-2, H-3	~3.5	~3.5	~3.5	~3.5
C-1, C-2	~45	~51		
C-1, C-3	~15	~15		
C-1, C-4	0	0		
C-1, C-5	0	0		
C-2, C-3	38.8	~39		
C-2, C-4	2.0	2.0		
C-2, C-5	0	2.4		

producing a complex multiplet that could not be interpreted (Table I). H-4 of **2p** partially overlapped this multiplet, but the remaining non-anomeric protons of **2p** were well resolved. The prochirality of the C-5 protons was assigned on the basis of $^3J_{H\text{-}4,H\text{-}5}$ (Table II). Because **2p** prefers the $^4C_1$ conformation, H-4 and H-5*S* are antiperiplanar and thus more strongly coupled than H-4 and H-5*R*, which are gauche[53].

Although **1o** and **1p** adopt both the $^4C_1$ and $^1C_4$ conformations, their prochiral C-5 protons could be assigned on the basis of $^3J_{H\text{-}4,H\text{-}5}$. H-4 and H-5*R* are gauche in both chair conformations and therefore not coupled as strongly as H-4 and H-5*S*, which are antiperiplanar in the $^4C_1$ conformation[53].

The chemical shifts of H-3–H-5 of **1g** and **2h** (Table III) are similar to those of the corresponding protons of the 2-pentulofuranoses[45]. The prochiralities of the C-5 protons were assigned on the basis of their relative chemical shifts; in the D series, H-5*S* is more shielded by O-4 than H-5*R* (ref. 41). The intensities of the proton signals of **1g**, **1m**, and **1n** were similar, but these signals could be differentiated by the use of several parameters. Thus $^2J_{H\text{-}5R,H\text{-}5S}$ in **1g** (Table IV) is much smaller[41,45] than $^2J_{H\text{-}5R,H\text{-}5S}$ in **1m** and **1n** (Table VIII), which prefer the $^1C_4$ conformation[53]. H-3 (and H-4) of **1m** and **1n** are strongly deshielded by the free carbonyl group[45], and thus resonate at a much lower field than H-3 and H-4 of **1g**.

In the $^1C_4$ conformation, the anomeric protons of **1m** and **1n** are equatorial and

axial, respectively, and these anomeric protons were assigned on the basis of $^1J_{C\text{-}1,H\text{-}1}$ (Table III)[37–39]. The anomeric proton of **1m** is moderately coupled to H-3, permitting the assignment of the latter proton. Signals for a pair of C-5 protons (H-5*R* and H-5*S*) were observed at 4.04–4.09 p.p.m. (Table VII), and signal intensities and the magnitudes of coupling constants suggested that these protons belonged either to **1m** or **1n**. The values of $^3J_{C\text{-}1,H\text{-}5}$ obtained from the ^{1}H-coupled ^{13}C-spectrum of the 1-^{13}C-substituted compound support their assignment to **1m**.

The remaining proton signals of **1m** and **1n** could not be assigned unequivocally without two-dimensional ^{1}H-n.m.r. spectroscopy. H-4 of **1m**, and H-4 and H-5*R* of **1n**, produce the three-proton multiplet at ~4.45 p.p.m. (Table VII). H-5*R* of **1n** resonates at a lower field than H-5*R* of **1m** due to the deshielding effect of the axial O-1 (refs. 54, 55). H-5*S* of **1n** resonates upfield from H-5*S* of **1m**, the latter being deshielded by the equatorial O-1 (ref. 53).

The signal for H-1 of **1n** is found at higher field than that of H-1 of **1m** (Table VII) despite the fact that equatorial anomeric protons normally resonate at lower fields than axial anomeric protons[53–55]. The unusual behavior of H-1 of **1n** may be due to the strong shielding effect of the coplanar carbonyl group[56a].

The anomeric proton of the minor aldofuranose endocyclic hydrate **1k** was coupled to H-3, allowing these proton signals to be correlated to the same structure (Tables V and VI). Knowledge of $^3J_{H\text{-}3,H\text{-}4}$ was used to locate the H-4 multiplet, and H-5*R* and H-5*S* were located using $^3J_{H\text{-}4,H\text{-}5}$. The prochirality of the C-5 protons of **1k** was assigned by analogy to assignments made for the structurally related methyl D-pento-

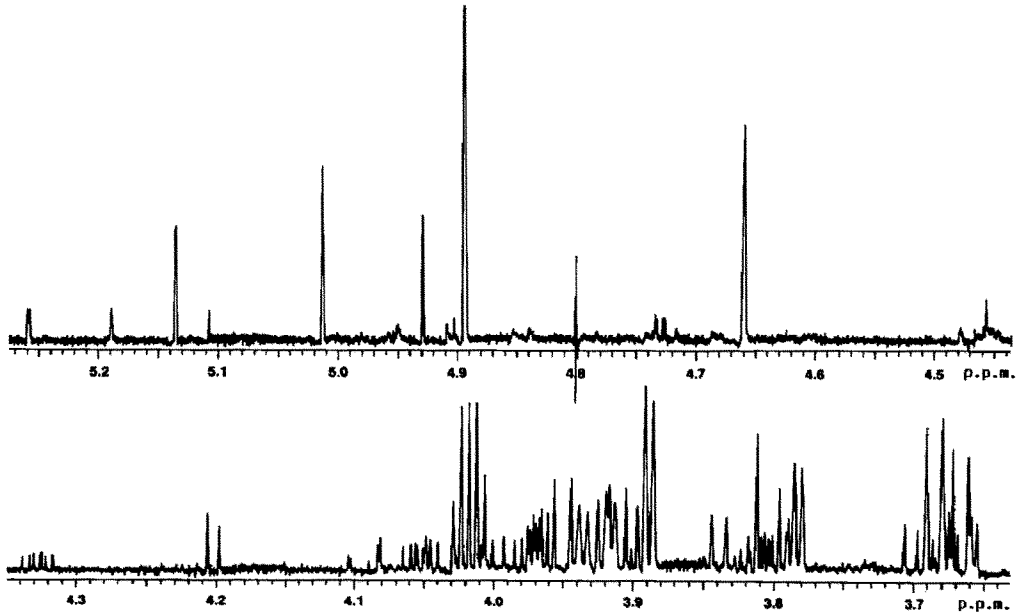

Fig. 4. ^{1}H-N.m.r. spectrum (620 MHz) of D-*erythro*-pentos-2-ulose (**1**) at ambient temperature.

furanosides[41,56b]; H-5*R* resonated upfield of H-5*S* and the former was coupled more strongly to H-4 than the latter.

H-3 of the major aldofuranose endocyclic hydrate **1l** gave a symmetric doublet at 3.95 p.p.m. (Table V, Fig. 4). Two-dimensional ^{1}H-n.m.r. spectroscopy of **1** showed that H-4 and H-5*S* of **1l** resonate at 3.79–3.83 p.p.m., giving a complex non-first-order multiplet, whereas the H-5*R* quartet of **1l** appears at 3.68 p.p.m. and is completely overlapped with the more intense H-5*S* quartet of **1p**.

Two-dimensional ^{1}H-n.m.r. spectra of the pentos-2-uloses. — The two-dimensional ^{1}H-n.m.r. techniques used in this study included DQF-COSY (analysis of **1**) and homonuclear 2D *J*-spectroscopy (analysis of **1**, D-(1-^{13}C)*erythro*-pentos-2-ulose and D-(2-^{13}C)*erythro*-pentos-2-ulose). Experimental parameters for the DQF-COSY were set to detect cross-peaks for protons having $J_{H,H} \geqslant 3$ Hz. This initial setting eliminated some of the possible cross-peaks, but the DQF-COSY spectrum of **1** was still very complicated (data not shown), due to severely overlapping signals, especially in the 3.65–4.10 p.p.m. region.

The DQF-COSY, homonuclear 2D *J*, and one-dimensional n.m.r. data for **1** were compatible, but generally it was not possible to make structural assignments on the basis of DQF-COSY alone. The DQF-COSY spectrum of **1**, however, gave important complementary structural data for isomers which had some of their non-anomeric protons resonating outside the crowded 3.65–4.10 p.p.m. region. Thus, the assignment of the H-3–H-5 protons of **1g** was straightforward, whereas in the one-dimensional spectrum the H-5*S* quartet of **1g** overlapped with more intense proton signals.

The DQF-COSY data also allowed the assignment of the H-4 protons of **1m** and **1n** to the multi-proton multiplet at ~4.55 p.p.m., on the basis of coupling between H-3 and H-4. The values of $^3J_{H\text{-}4,H\text{-}5R}$ and $^3J_{H\text{-}4,H\text{-}5S}$ in **1m** and **1n** were very small ($^1C_4$ conformation), and therefore no cross peaks were observed between H-4 and H-5*R*, and H-4 and H-5*S*. However, the large magnitude $^2J_{H\text{-}5R,H\text{-}5S}$ enabled the assignment of H-4*R* and H-5*S* of **1n** (4.57 and 3.85 p.p.m., respectively).

The homonuclear 2D *J*-spectrum of **1** gave chemical shifts and coupling constants similar to those determined from the one-dimensional ^{1}H-spectrum of **1**. Determination of these parameters from the homonuclear 2D *J*-spectrum is, however, more straightforward because chemical shifts and coupling constants are observed in different dimensions, and signal overlappings are significantly reduced. Thus, it was possible to completely resolve the H-4 and H-5*S* multiplets of **1l** (Fig. 5), and the H-4 and H-5*R* multiplets of **1n**. Other multiplets which overlapped in one-dimensional ^{1}H-n.m.r. but were resolved in the homonuclear 2D *J*-spectrum included H-5*S* of **1g**, H-4 of **1m**, and H-5*S* of **1n**.

The H-5*R* quartet of **1l** was the only proton multiplet from the seven major isomers of **1** that could not be identified in the homonuclear 2D *J*-spectrum of **1**. This signal was, however, observed in the homonuclear 2D *J*-spectrum of D-(1-^{13}C)*erythro*-pentos-2-ulose (Fig. 6). In this experiment, ^{13}C–^{1}H couplings are observed in the same dimension as ^{1}H chemical shifts (Fig. 6). Thus, for example, H-5*S* of the 1-^{13}C-labeled **1p** gave two quartets which were separated by $^3J_{C\text{-}1,H\text{-}5S}$ (4.7 Hz). The splitting of the H-5*S*

quartet of **1p** revealed an underlying quartet with similar ^1H–^1H coupling constants. On the basis of $^2J_{H\text{-}5R,H\text{-}5S}$, this quartet was assigned to the missing H-5*R* multiplet of **1l**.

Generally, homonuclear 2D *J*-spectroscopy of D-(1-^{13}C)*erythro*-pentos-2-ulose and D-(2-^{13}C)*erythro*-pentos-2-ulose afforded a straightforward way of determining ^{13}C–^1H coupling constants. The advantages of this method were most apparent in cases of overlapping and non-first-order multiplets in one-dimensional experiments. This method of extracting ^{13}C–^1H coupling constants in crowded regions of spectra may be valuable in studies of other complex molecules. Homonuclear 2D *J*-spectra also revealed additional fine-splitting due to long-range ^1H–^1H couplings, especially in pyranoid structures (Fig. 5).

Conformational properties. — (a) Pyranose hydrates. The relative free energies of the chair conformations of the pyranose endocyclic hydrates **1o**, **1p**, **2o**, and **2p** can be calculated as described by Angyal[46]. The magnitude of the anomeric effect is somewhat uncertain; an average value of 0.80 kcal.mol^{-1} was used in these calculations.

The calculated free energies indicate that the predominant conformation of **2o** and **2p** is $^4C_1$, and that **2o** should be more abundant than **2p**. The experimental data agree with these predictions. Preference for the $^4C_1$ conformation of **2p** is supported by the large values of $^3J_{H\text{-}3,H\text{-}4}$, $^3J_{H\text{-}4,H\text{-}5R}$, and $^3J_{H\text{-}4,H\text{-}5S}$ (ref. 53) (Table II). The assignment of configuration **2o** to the more abundant pyranose hydrate anomer is substantiated by the larger $^1J_{C\text{-}1,H\text{-}1}$ (refs. 37–39), the more shielded C-3 and C-5 signals (shielding by axial O-1)[52], and the chemical shifts of H-1, H-3, and H-5*S* (deshielded by axial O-1), compared to corresponding parameters for **2p** (Table I)[54,55].

Calculated conformational free energies[46] suggest that the β anomer **1p** is more

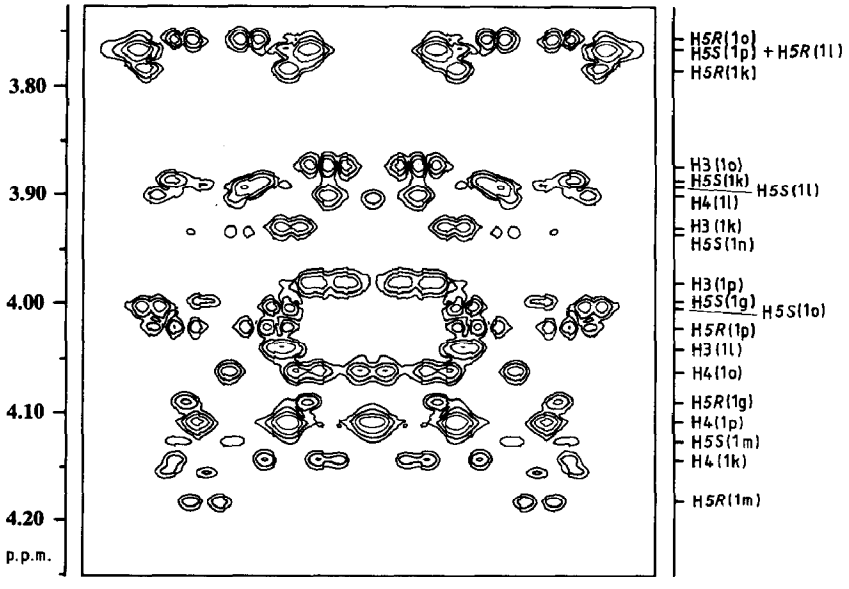

Fig. 5. Partial homonuclear 2D *J*-spectrum (500 MHz) of D-*erythro*-pentos-2-ulose (**1**) at 30°, showing some of the non-anomeric ^1H-signal assignments for the seven major tautomers.

stable than the α anomer **1o**. In the *erythro* isomers, the $^4C_1$ and $^1C_4$ conformers have comparable stabilities. The conformational equilibrium may be assessed experimentally in several ways. In particular, $^3J_{H\text{-}4,H\text{-}5S}$ is useful because H-4 and H-5*S* are antiperiplanar in $^4C_1$ and gauche in $^1C_4$. In $^4C_1$, $^3J_{H\text{-}4,H\text{-}5S}$ is ~10.5 Hz, whereas in $^1C_4$ it is ~1.8 Hz[53,57,58]. On the basis of the observed values of $^3J_{H\text{-}4,H\text{-}5S}$, **1o** and **1p** exist as $^4C_1$ and $^1C_4$ conformers in ratios of 37:63 and 57:43, respectively. A similar calculation may be performed with $^3J_{H\text{-}4,H\text{-}5R}$ using values of 5.5 and 1.3 Hz for the $^4C_1$ and $^1C_4$ conformers, respectively; estimated ratios of $^4C_1$ and $^1C_4$ conformers in **1o** and **1p** are then 33:67 and 55:45, respectively, in good agreement with ratios based on $^3J_{H\text{-}4,H\text{-}5S}$.

Conformational equilibria may also be determined from $^3J_{C\text{-}1,H\text{-}5R}$ and $^3J_{C\text{-}1,H\text{-}5S}$.

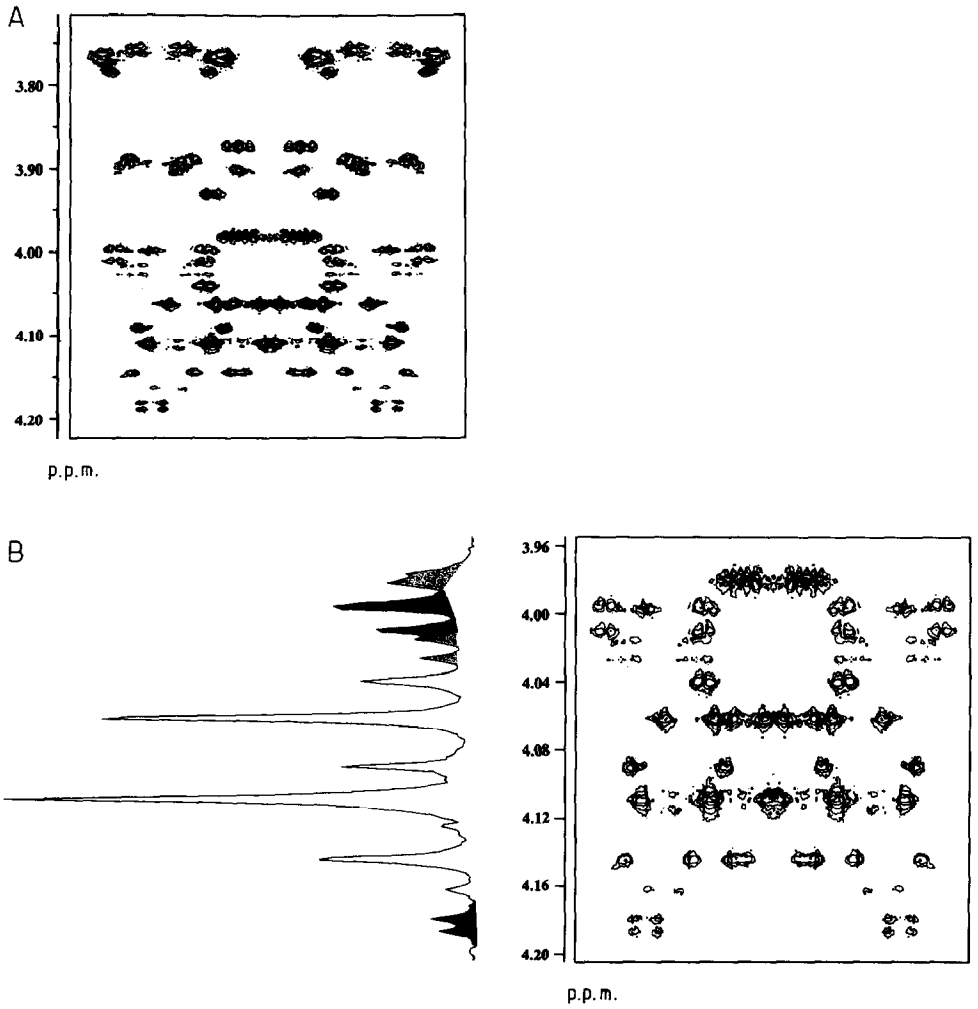

Fig. 6. A. Partial homonuclear 2D *J*-spectrum (500 MHz) of D-(1-^{13}C)*erythro*-pentos-2-ulose at 30°. B. An expanded region of A, showing additional contour splittings caused by ^{13}C–^{1}H spin-coupling. The projected spectrum reveals four doublets from protons spin-coupled to ^{13}C at C-1: H-5*R* of **1m**, 4.18 p.p.m.; H-5*R* of **1p**, 4.02 p.p.m.; H-5*S* of **1o**, 4.00 p.p.m.; and H-3 of **1p**, 3.98 p.p.m.

Standard values of $^3J_{C\text{-}1,H\text{-}5}$ are: 10.0 Hz when O-1 and H-5 are equatorial; 2.9 Hz when O-1 is equatorial and H-5 is axial; 7.0 Hz when O-1 is axial and H-5 is equatorial; and 2.0 Hz when O-1 and H-5 are axial[59–62]. Using these values, **1o** is calculated to exist in $^4C_1$ and $^1C_4$ conformations in a ratio of 32:68 (from $^3J_{C\text{-}1,H\text{-}5R}$) or 34:66 (from $^3J_{C\text{-}1,H\text{-}5S}$). Similarly **1p** adopts the $^4C_1$ and $^1C_4$ conformations in a ratio of 51:49 (from $^3J_{C\text{-}2,H\text{-}5R}$) or 56:44 (from $^3J_{C\text{-}1,H\text{-}5S}$).

The conformational equilibrium of **1o** may be determined from an analysis of $^2J_{C\text{-}2,H\text{-}1}$. Standard values for this coupling are obtained from **2o** and **2p**, which are conformationally homogeneous. When H-1 is equatorial, $^2J_{C\text{-}2,H\text{-}1} = 2.7$ Hz, but 4.2 Hz when H-1 is axial. These couplings have opposite signs. If the observed $^2J_{C\text{-}2,H\text{-}1}$ in **1o** and the larger standard value are assumed to have the same sign, then **1o** is found to exist as $^4C_1$ and $^1C_4$ conformers in a 35:65 ratio. The magnitude of $^2J_{C\text{-}2,H\text{-}1}$ in **1p** should be 0.3 Hz if the $^4C_1$:$^1C_4$ ratio is 56:44 as suggested from $^3J_{C\text{-}1,H\text{-}5}$. The observed zero value of $^2J_{C\text{-}2,H\text{-}1}$ is consistent with this predicted value.

Thus, three methods based on ^{1}H–^{1}H and ^{13}C–^{1}H couplings give similar estimates of the conformational equilibria of the *erythro* isomers; data may be averaged to give relative populations of $^4C_1$ and $^1C_4$ conformers of 34:66 for **1o** and 56:44 for **1p**. It should be noted that $^1J_{C\text{-}1,H\text{-}1}$ and $^1J_{C\text{-}1,C\text{-}2}$ in **1o** and **1p** are similar in magnitude (Table II), suggesting the presence of conformational equilibria[37–39], although accurate $^4C_1$:$^1C_4$ ratios cannot be calculated solely on the basis of these couplings.

The observed ^{13}C chemical shifts of **1o** and **1p** may be evaluated in terms of conformational equilibria using the ^{13}C chemical shifts of **2o** and **2p** as standards and adding the effects of an axial O-3 or O-4 to these latter values[52,54,55]. The large differences between the calculated chemical shifts of some carbons in the two chair conformers of **1o** and **1p** then permit the conformational equilibria to be calculated with reasonable accuracy. For example, the observed value of $\delta_{C\text{-}3}$ of **1o** is 73.3 p.p.m.; in the $^4C_1$ and $^1C_4$ conformers, $\delta_{C\text{-}3}$ is calculated to be 70.5 and 74.9 p.p.m., respectively[52], giving a 36:64 ratio of the conformers. The observed value of $\delta_{C\text{-}4}$ of **1o** (69.2 p.p.m.) gives a 44:56 ratio of $^4C_1$ and $^1C_4$ when standard values for $\delta_{C\text{-}4}$ of 67.0 p.p.m. ($^4C_1$) and 70.4 p.p.m. ($^1C_4$) are used in the calculation. Similar calculations based on $\delta_{C\text{-}4}$ indicate that **1p** exists as $^4C_1$ and $^1C_4$ conformers in a 53:47 ratio.

(b) Unhydrated pyranoses. The unhydrated pyranoses **1m**, **1n**, **2m**, and **2n** are conformationally homogeneous, as suggested from the large difference in $^1J_{C\text{-}1,H\text{-}1}$ between α and β anomers (Table VIII)[37–39]. The *threo* isomers **2m** and **2n** prefer the $^4C_1$ conformation; the $^1C_4$ conformer of **2n** is destabilized by a *syn* interaction between O-1 and O-3. This conformational assignment is substantiated by zero couplings between C-1 and H-3 (Table VIII).

Zero couplings between C-1 and H-3 in the *erythro* isomers **1m** and **1n** indicate that these compounds prefer the $^1C_4$ conformation. The coupling constants $^3J_{H\text{-}4,H\text{-}5R}$ and $^3J_{H\text{-}4,H\text{-}5S}$ in **1m** and **1n** were very small, indicating a low abundance of the $^4C_1$ conformer[53,57,58]. The geminal coupling, $^2J_{H\text{-}5R,H\text{-}5S}$, is -13.1 ± 0.2 Hz, typical of $^1C_4$ conformers of aldopentopyranoses and ketohexopyranoses[53,58,63].

The values of $^3J_{C\text{-}1,H\text{-}5R}$ and $^3J_{C\text{-}1,H\text{-}5S}$ in the pentos-2-ulopyranoses also indicate a

preference for one chair conformation[59–62]. The analogous $^3J_{C\text{-}1,H\text{-}5}$ couplings in **1m** and **2n** are very similar, whereas there are significant differences between the analogous $^3J_{C\text{-}1,H\text{-}5}$ couplings in **1n** and **2m**. The latter differences might be explained if **2m** exists to the extent of ~10% in the $^1C_4$ conformation.

Using the relative populations of unhydrated and hydrated pyranoses, and the conformational free energies[46] of the pyranose hydrates as reference values, **1m** and **1n** were calculated to be more stable than **2m** and **2n** (ΔG° = 0.6 kcal.mol^{-1}). This result suggests that the unhydrated pyranose is stabilized by an axial O-4, possibly *via* an attractive electrostatic interaction between O-4 and the strongly polarized carbonyl group at C-2. Interestingly, the α and β anomers are equally stable, suggesting that the anomeric effect in **1m** and **2n** is largely compensated by a stabilizing interaction between O-1 and O-2; this stabilizing interaction is probably intramolecular hydrogen bonding. It is believed that hydrogen bonding in α-hydroxyketones negates the α-halo effect, which favors a *gauche* orientation of the electronegative substituent and the carbonyl oxygen[64]. On the basis of these electrostatic interactions and the usual nonbonded interactions (including the anomeric effect)[46], the *α-threo* isomer **2m** is predicted to assume the less favoured $^1C_4$ conformation, and this prediction is supported experimentally by the value of $^3J_{C\text{-}1,H\text{-}5}$.

(c) Ketofuranose exocyclic hydrates. The rotamer populations of the dihydroxymethyl group [-CH(OH)$_2$] in ketofuranose exocyclic hydrates **1g**, **1h**, **2g**, and **2h** can be evaluated from $^2J_{C\text{-}2,H\text{-}1}$ (Table IV). Standard values are provided by the corresponding coupling constants in **2o** and **2p** (Table II). The magnitude of $^2J_{C\text{-}2,H\text{-}1}$ is 2.7 Hz when H-1 and C-3 are antiperiplanar and 4.2 Hz when these atoms are *gauche*. These two couplings have opposite signs. In **1g** and **2h**, no coupling is observed between H-1 and C-2, suggesting that *t* (H-1 and C-3 trans) is the most abundant rotamer. In **1h**, $^2J_{C\text{-}2,H\text{-}1}$ = 1.2 Hz; because the coupling signs were not determined, two combinations of rotamer populations are consistent with this value. The more probable combination is 45% *t*, and 55% *g* in which H-1 and O-3 are *syn*. In the alternative *g* rotamer, a destabilizing *syn* interaction exists between O-1*R* and O-3. Because of the preferred *syn* orientation of H-1 and O-3 in **1h**, H-1 is more deshielded than H-1 in **1g** (Table III).

The chemical shifts and ^{1}H–^{1}H coupling data for the ring protons of **1g** and **2h** are very similar to those for α-D-*erythro*-2-pentulofuranose[45] and β-D-*threo*-2-pentulofuranose, respectively, with the exception of $\delta_{H\text{-}3}$. H-3 in both **1a** and **2h** resonates downfield from H-3 of the corresponding 2-pentulofuranoses, possibly because of the deshielding effect of O-1*R* and O-1*S*. The ring conformations of the configurationally related 2-pentulofuranoses and exocyclic 2-pentulofuranose hydrates are very similar.

(d) Aldofuranose endocyclic hydrates. The magnitudes of $^1J_{C\text{-}1,H\text{-}1}$ in the aldofuranose endocyclic hydrates **1k**, **1l**, **2k**, and **2l** were relatively large (Table VI), indicating a preference for conformers having quasi-axial anomeric hydroxyl groups[40]. This conformational preference explains the larger $^3J_{C\text{-}1,H\text{-}3}$ in **1k** and **2l** compared to $^3J_{C\text{-}1,H\text{-}3}$ in **1l** and **2k**. This difference in $^3J_{C\text{-}1,H\text{-}3}$ was used to assign anomeric configuration. The remaining ^{13}C and ^{1}H signals of **1k** and **1l** were assigned on the basis of signal intensities (Table V).

It is useful to compare the conformations of the aldofuranose endocyclic hydrates

to those of the structurally related aldopentofuranoses and their methyl glycosides[40,41,56b]. Unfortunately, the aldofuranose endocyclic hydrates contain only one $^3J_{H,H}$ ($^3J_{H\text{-}3,H\text{-}4}$) that is useful for assessing ring conformation. In the *α-erythro* isomer **1k**, $^3J_{H\text{-}3,H\text{-}4}$ = 6.4 Hz, which is similar to the corresponding value in methyl α-D-arabinofuranoside (5.9 Hz) but very different from $^3J_{H\text{-}3,H\text{-}4}$ in methyl α-D-ribofuranoside (3.3 Hz)[41]. α-D-Arabinofuranose and α-D-ribofuranose are puckered significantly at the ring oxygen and C-2, respectively[41]. In α-D-arabinofuranose, puckering at the ring oxygen eliminates an unfavorable *syn* interaction between O-2 and C-5. Since this interaction is also possible in **1k**, it is not surprising that its ring conformation is similar to that of α-D-arabinofuranose, as suggested by $^3J_{H\text{-}3,H\text{-}4}$. The values for $^3J_{H\text{-}3,H\text{-}4}$ in **1l**, methyl β-D-arabinofuranoside, and methyl β-D-ribofuranoside are very similar, indicating that these structures prefer ring conformations puckered at C-2 (ref. 41).

The ring conformations of the aldofuranose endocyclic hydrates may also be assessed from the magnitudes of $^2J_{C\text{-}2,H\text{-}3}$. Standard values obtained from the coupling data for the pentos-2-ulopyranose hydrates are 2.0 Hz and 5.2 Hz when O-3 and H-3, respectively, are antiperiplanar to C-1. In **1k**, $^2J_{C\text{-}2,H\text{-}3}$ = 3.3 Hz, which is consistent with an ^OE conformation. The small $^2J_{C\text{-}2,H\text{-}3}$ in **1l** suggests a predominance of $^1T_2$ or $^3T_2$ conformations. The $^3T_2$ conformer, however, seems more probable because C-1 is not coupled to H-3 and H-4, and because $^3J_{H\text{-}3,H\text{-}4}$ in **1l** is larger than $^3J_{H\text{-}3,H\text{-}4}$ in **1k**.

An analysis of $^2J_{C\text{-}2,H\text{-}3}$ (3.5 and 4.2 Hz) also permitted an assignment of the C-2 signals of **2k** and **2l**. The signal with the larger coupling was assigned to **2l** because the alternative assignment is consistent with ^4E or E_O conformers, in disagreement with the other coupling data. The conformations preferred by **2l** are $^3T_2$ or $^3T_4$, in which the exocyclic hydroxymethyl group is quasi-equatorial and the torsion angle between this hydroxymethyl group and O-3 is relatively large. These conformations are consistent with the observed zero couplings between C-1 and H-4, and between C-2 and H-4.

On the basis of $^2J_{C\text{-}2,H\text{-}3}$ in **2k**, this furanose ring appears to prefer the $^OT_4$ or ^OE conformations. These conformations are consistent with the zero couplings between C-1 and H-4 and C-2 and H-4, and the observed coupling between C-1 and H-3.

Equilibrium composition of the pentos-2-uloses. — The solution compositions of the pentos-2-uloses (Table IX) are determined by the same factors that affect the equilibrium compositions of aldopentoses and ketopentoses[12]. Pyranoid structures dominate, though not as strongly as for the aldopentoses. Furanose forms are relatively stable when no *cis* interactions occur between vicinal hydroxyl and hydroxymethyl (or dihydroxymethyl) groups. The proportion of acyclic forms is low; in the present study unequivocal evidence for the presence of acyclic forms was not obtained. The greatest difference in equilibrium composition between pentos-2-uloses and simple aldopentoses is the presence of dimeric forms. In the former case the furanoid and pyranoid monomers may dimerize, whereas aldopentoses dimerize only *via* their acyclic forms, which are present in low abundance in aqueous solution.

The hydration constants of the pentos-2-ulopyranoses and pentos-2-ulofuranoses are very large. Although it is difficult to find suitable reference data, the hydration constants of the pentos-2-ulo-2,5-furanoses at 80° are larger than the second hydration

constant of glyoxal[4], and ~20–30 times larger than the hydration constant of glyceraldehyde[42]. The hydration constants of pentos-2-ulopyranoses at 25° are 20–300 times larger than the hydration constant of dihydroxyacetone[4]. It is noteworthy that the hydrates of 2-ketopentoses and 2-ketohexoses have not yet been detected.

The extensive hydration of the pentos-2-uloses is partly due to the effect of the α oxygen atom on the electrophilicity of the carbonyl carbon, but there is also evidence that cyclic ketones are hydrated more easily than acyclic ketones even though the carbonyl carbons are equally electrophilic. For example, 1,2:5,6-di-*O*-isopropylidene-α-D-*ribo*-hexos-3-ulofuranose has been isolated as its hydrate[66,67], and the ^{13}C-n.m.r. spectrum of calcium D-*threo*-2,5-hexodiulosonate[68] indicates that the α-pyranose hydrate is the major component, whereas little or no keto component is present. D-*erythro*-Pentos-4-ulose also exists mainly as pyranose hydrates[69].

The stabilities of the bisulfite adducts of aldos-2-uloses and their cyclic derivatives[8,36] are compatible with the large hydration constants of the pentos-2-uloses. If steric effects are ignored, the ratio of bisulfite adduct to its corresponding hydrate is expected to be constant and independent of the structure of the carbonyl compound. Thus, the proportion of the bisulfite adduct is greatest when the degree of hydration (in the absence of hydrogen sulfite) is highest. The degree of hydration depends not only on the relative stabilities of the hydrate and the carbonyl structure, but also on the stabilities of the possible ring structures. From these considerations, it appears that previous arguments supporting the presence of the structure with an exocyclic C-1 (refs. 8, 36) are not valid.

CONCLUSIONS

The equilibrium compositions of the pentos-2-uloses have been determined for the first time by n.m.r. spectroscopy. The large number of different structures compli-

TABLE IX

Normalized equilibrium populations of monomeric forms of D-pentos-2-uloses in deuterium oxide at two temperatures

Tautomer	*Proportion (%)*			
	erythro		threo	
	25°	*80°*	*25°*	*80°*
α-Aldopyranose endocyclic hydrate	20.5	14.0	59.8	40.8
β-Aldopyranose endocyclic hydrate	38.8	24.2	29.1	26.1
α-Aldofuranose endocyclic hydrate	10.9	12.2	1.5	3.3
β-Aldofuranose endocyclic hydrate	14.2	14.0	1.3	2.8
α-Ketofuranose exocyclic hydrate	5.2	7.1	1.0	2.2
β-Ketofuranose exocyclic hydrate	1.1	1.6	5.4	10.4
α-Aldopyranose	4.5	24.2	0.9	7.1
β-Aldopyranose	4.5		1.0	6.5
Other carbonyl structures	0.3	2.7	0.0	0.8

cated the analysis, but significant simplification was achieved by the use of ^{13}C-substitution at the anomeric carbons to facilitate signal assignments and allow measurement of valuable ^{13}C–^{1}H and ^{13}C–^{13}C spin-coupling constants. Structural assignments have been made primarily on the basis of the chemical shifts of the enriched carbons (C-1 and C-2) and from ^{13}C–^{1}H coupling data.

In the present work eight forms of the D-*erythro*- and D-*threo*-pentos-2-uloses were identified with confidence. The relative populations of the least abundant forms were ~1%. The detection and assignment of forms present at <1% will require purer preparations and elevated temperatures, but these studies will be hampered by degradation of the heat-labile pentos-2-uloses.

The conformational analysis of the furanose and pyranose forms of the pentos-2-uloses has been based primarily on ^{1}H–^{1}H and ^{13}C–^{1}H coupling constants, although ^{1}H and ^{13}C chemical shifts and ^{13}C–^{13}C coupling constants were also useful. For D-*erythro*-pentos-2-ulopyranose hydrates, internally consistent assignments were obtained from $^{3}J_{H,H}$, $^{3}J_{C,H}$, and $^{2}J_{C,H}$ values and ^{13}C chemical shifts. This example points clearly to the utility of integrated n.m.r. data to decipher a relatively complex conformational puzzle.

The conformational stabilities of the furanose and pyranose hydrates of the pentos-2-uloses were determined using parameters derived for simple aldoses and ketoses. Pentos-2-ulopyranoses favor conformations having axial anomeric hydroxyl groups and minimal 1,3-diaxial interactions. The furanose hydrates prefer conformers having quasi-axial anomeric hydroxyl groups and quasi-equatorial exocyclic hydroxymethyl or dihydroxymethyl groups. The conformational stabilities of unhydrated pentos-2-ulopyranoses are affected not only by the anomeric effect and the usual steric interactions, but also by intramolecular hydrogen bonding between the carbonyl oxygen and vicinal equatorial hydroxyl groups, and by electrostatic interactions between an axial O-4 and the carbonyl group.

ACKNOWLEDGMENTS

This work was supported by the National Institutes of Health (GM 33791), the Research Corporation (10028), the Academy of Finland, and Omicron Biochemicals, Inc. The NMR Facility for Biomedical Studies (Carnegie–Mellon) is partly supported by NIH grant P41RR00292.

REFERENCES

1 J. W. Green, in W. Pigman and D. Horton (Eds.), *The Carbohydrates, Chemistry and Biochemistry*, Vol. IB, 2nd edn., Academic Press, New York, 1980, pp. 1101–1166.
2 E. F. L. J. Anet, *Adv. Carbohydr. Chem.*, 19 (1964) 181–218.
3 W. Pigman and E. F. L. J. Anet, in W. Pigman and D. Horton (Eds.), *The Carbohydrates, Chemistry and Biochemistry*, Vol. IA, 2nd edn., Academic Press, New York, 1972, pp. 165–194.
4 T. Vuorinen, *Ann. Acad. Sci. Fennicae, Ser. Q*, II (1988) no. 220.
5 (a) E. Sjöström, *Wood Chemistry, Fundamentals and Applications*, Academic Press, New York, 1981, pp. 104–168; (b) T. C. Crawford and S. A. Crawford, *Adv. Carbohydr. Chem. Biochem.*, 37 (1980) 79–155.
6 F. Petuely, *Monatsh.*, 83 (1952) 765.

7 S. Bayne and J. A. Fewster, *Adv. Carbohydr. Chem.*, 11 (1956) 43–96.
8 O. Theander, in W. Pigman and D. Horton (Eds.), *The Carbohydrates, Chemistry and Biochemistry*, Vol. IB, 2nd edn., Academic Press, New York, 1980, pp. 1013–1099.
9 P. A. G. Ruiz, I. C. Travesedo, and A. S. Martinez, *Can. J. Chem.*, 62 (1984) 870–877.
10 F. Barba, P. A. Garcia, A. Guirado, and A. Zapata, *Carbohydr. Res.*, 105 (1982) 158–164.
11 A. A. El-Dash and J. E. Hodge, *Carbohydr. Res.*, 18 (1971) 259–267.
12 S. J. Angyal, *Adv. Carbohydr. Chem. Biochem.*, 42 (1984) 15–68.
13 J. Havlicek, G. Petersson, and O. Samuelson, *Acta Chem. Scand.*, 26 (1972) 2205–2215.
14 A. S. Serianni, J. Pierce, S.-G. Huang, and R. Barker, *J. Am. Chem. Soc.*, 104 (1982) 4037–4044.
15 J. Pierce, A. S. Serianni, and R. Barker, *J. Am. Chem. Soc.*, 107 (1985) 2448–2456.
16 W. J. Goux, *J. Am. Chem. Soc.*, 107 (1985) 4320–4327.
17 J. R. Snyder and A. S. Serianni, *J. Org. Chem.*, 51 (1986) 2694–2702.
18 S. R. Maple and A. Allerhand, *J. Am. Chem. Soc.*, 109 (1987) 3168–3169.
19 J. R. Snyder and A. S. Serianni, *Carbohydr. Res.*, 163 (1987) 169–188.
20 J. R. Snyder and A. S. Serianni, *Carbohydr. Res.*, 166 (1987) 85–99.
21 J. R. Snyder, E. R. Johnston, and A. S. Serianni, *J. Am. Chem. Soc.*, 111 (1989) 2681–2687.
22 R. Z. Weidenhagen, *Wirtschaftsgruppe Zuckerind.*, 87 (1937) 711.
23 L. L. Salomon, J. J. Burns, and C. G. King, *J. Am. Chem. Soc.*, 74 (1952) 5161–5162.
24 F. H. H. Carlsson, A. J. Charlson, and E. C. Watton, *Carbohydr. Res.*, 36 (1974) 359–368.
25 E. C. Taylor and P. A. Jacobi, *J. Am. Chem. Soc.*, 98 (1976) 2301–2307.
26 P. A. Jacobi and M. Martinelli, *J. Org. Chem.*, (1981) 5416–5418.
27 J. Volc, P. Sedmera, and V. Musilek, *Collect. Czech. Chem. Commun.*, 45 (1980) 950–955.
28 T.-N. E. Liu, B. Wolf, J. Geigert, S. L. Neidleman, J. D. Chin, and D. S. Hirano, *Carbohydr. Res.*, 113 (1983) 151–157.
29 (a) J. E. Hodge and B. T. Hofreiter, *Methods Carbohydr. Chem.*, 1 (1962) 380–394; (b) S. J. Angyal, G. S. Bethell, and R. J. Beveridge, *Carbohydr. Res.*, 73 (1979) 9–18.
30 J. K. N. Jones and R. A. Wall, *Can. J. Chem.*, (1960) 2290–2294.
31 T. Vuorinen, *Carbohydr. Res.*, 127 (1984) 319–325.
32 A. I. A. Vogel, *Textbook of Quantitative Inorganic Analysis, Including Elementary Instrumental Analysis*, 3rd edn., Wiley, New York, 1961, p. 363.
33 M. A. Madson and M. S. Feather, *Carbohydr. Res.*, 94 (1981) 183–191.
34 G. Petersson, *Carbohydr. Res.*, 33 (1974) 47–61.
35 O. Samuelson, *Methods Carbohydr. Chem.*, 6 (1972) 65–75.
36 O. Theander, *Adv. Carbohydr. Chem.*, 17 (1962) 223–299.
37 K. Bock, I. Lundt, and C. Pedersen, *Tetrahedron Lett.*, (1973) 1037–1040.
38 K. Bock and C. Pedersen, *J. Chem. Soc., Perkin Trans. 2*, (1974) 293–297.
39 K. Bock and C. Pedersen, *Acta Chem. Scand., Ser. B*, 29 (1975) 258–264.
40 N. Cyr and A. S. Perlin, *Can. J. Chem.*, 57 (1979) 2504–2511.
41 A. S. Serianni and R. Barker, *J. Org. Chem.*, 49 (1984) 3292–3300.
42 L. Que and G. R. Gray, *Biochemistry*, 13 (1974) 146–153.
43 S. J. Angyal, G. S. Bethell, D. E. Cowley, and V. A. Pickles, *Aust. J. Chem.*, 29 (1976) 1239–1247.
44 S. J. Angyal and G. S. Bethell, *Aust. J. Chem.*, 29 (1976) 1249–1265.
45 T. Vuorinen and A. S. Serianni, unpublished data.
46 S. J. Angyal, *Aust. J. Chem.*, 21 (1968) 2737–2746.
47 R. U. Lemieux, T. L. Nagabhushan, and B. Paul, *Can. J. Chem.*, 50 (1972) 773–776.
48 J. A. Schwarcz and A. S. Perlin, *Can. J. Chem.*, 50 (1972) 3667–3676.
49 R. G. S. Ritchie, N. Cyr, B. Korsch, H. J. Koch, and A. S. Perlin, *Can. J. Chem.*, 53 (1975) 1424–1433.
50 S. J. Angyal and V. A. Pickles, *Aust. J. Chem.*, 25 (1972) 1711–1718.
51 E. Breitmaier and W. Voelter, *Carbon-13 NMR Spectroscopy, High-Resolution Methods and Applications in Organic Chemistry and Biochemistry*, 3rd edn., VCH, Weinheim, New York, 1987, pp. 215–222.
52 M. J. King-Morris and A. S. Serianni, *J. Am. Chem. Soc.*, 109 (1987) 3501–3508.
53 K. Bock and H. Thøgerson, *Annu. Rep. NMR Spectrosc.*, 13 (1982) 1–57.
54 G. Kotowycz and R. U. Lemieux, *Chem. Rev.*, 73 (1973) 669–698.
55 L. D. Hall, in W. Pigman and D. Horton (Eds.), *The Carbohydrates, Chemistry and Biochemistry*, Vol. IB, 2nd edn., Academic Press, New York, 1980, pp. 1299–1326.
56 (a) A. Nickon, M. A. Castle, R. Harada, C. E. Berkoff, and R. O. Williams, *J. Am. Chem. Soc.*, 85 (1963) 2185–2186; (b) S. J. Angyal, *Carbohydr. Res.*, 77 (1979) 37–50.

57 A. DeBruyn, M. Anteunis, and G. Verhegge, *Carbohydr. Res.*, 41 (1975) 295–297.
58 M. Budesinsky, M. Cerny, J. Dolezalova, M. Kulhanek, J. Pacak, and M. Tadra, *Collect. Czech. Chem. Commun.*, 49 (1984) 267–274.
59 J. A. Schwarcz and A. S. Perlin, *Can. J. Chem.*, 50 (1972) 3667–3676.
60 K. Bock and C. Pedersen, *Acta Chem. Scand., Ser. B*, 31 (1977) 354–358.
61 M. L. Hayes, A. S. Serianni, and R. Barker, *Carbohydr. Res.*, 100 (1982) 87–101.
62 G. D. Wu, A. S. Serianni, and R. Barker, *J. Org. Chem.*, 48 (1983) 1750–1757.
63 P. L. Durette, D. Horton, and J. D. Wander, in R. Gould (Ed.), *Carbohydrates in Solution*, Advances in Chemistry Series, 117, American Chemical Society, Washington, D.C., 1973, pp. 147–176.
64 E. L. Eliel, N. L. Allinger, S. J. Angyal, and G. A. Morrison, *Conformational Analysis*, Interscience Publishers, New York, 1965, p. 460.
65 S. J. Angyal and R. G. Wheen, *Aust. J. Chem.*, 33 (1980), 1001–1011.
66 O. Theander, *Acta Chem. Scand.*, 18 (1964) 2209–2216.
67 P. J. Beynon, P. M. Collins, and W. G. Overend, *Proc. Chem. Soc.*, (1964) 342–343.
68 T. C. Crawford, G. C. Andrews, H. Faubl, and G. N. Chmurny, *J. Am. Chem. Soc.*, 102 (1980) 2220–2225.
69 J. Srogl, M. Janda, I. Stibor, and J. Kucera, *Collect. Czech. Chem. Commun.*, 38 (1973) 455–458.